

Interfacial cracking in a graded coating/substrate system loaded by a frictional sliding flat punch

Hyung Jip Choi and Glaucio H. Paulino

Proc. R. Soc. A 2010 **466**, 853-880 first published online 16 November 2009
doi: 10.1098/rspa.2009.0437

Supplementary data

"Data Supplement"

<http://rspa.royalsocietypublishing.org/content/suppl/2009/11/13/rspa.2009.0437.DC1.html>

References

This article cites 36 articles, 2 of which can be accessed free

<http://rspa.royalsocietypublishing.org/content/466/2115/853.full.html#ref-list-1>

Subject collections

Articles on similar topics can be found in the following collections

[mechanical engineering](#) (104 articles)

[structural engineering](#) (26 articles)

[civil engineering](#) (17 articles)

Email alerting service

Receive free email alerts when new articles cite this article - sign up in the box at the top right-hand corner of the article or click [here](#)

To subscribe to *Proc. R. Soc. A* go to: <http://rspa.royalsocietypublishing.org/subscriptions>

Interfacial cracking in a graded coating/substrate system loaded by a frictional sliding flat punch

BY HYUNG JIP CHOI^{1,*} AND GLAUCIO H. PAULINO²

¹*School of Mechanical and Automotive Engineering, Kookmin University, Seoul 136-702, Republic of Korea*

²*Department of Civil and Environmental Engineering, University of Illinois at Urbana-Champaign, Urbana, Illinois 61801, USA*

An analysis of a coupled plane elasticity problem of crack/contact mechanics for a coating/substrate system with functionally graded properties is performed, where the rigid flat punch slides over the surface of the coated system that contains a crack. The graded material is treated as a non-homogeneous interlayer between dissimilar, homogeneous phases of the coated medium and the crack is assumed to exist along the interface between the interlayer and the substrate. Based on the Fourier integral transform method and the transfer matrix approach, formulation of the current coupled mixed boundary value problem lends itself to the derivation of a set of three simultaneous Cauchy-type singular integral equations. In the numerical results, the emphasis is placed on the investigation of interactions between the contact stress field and the crack-tip behaviour for various combinations of material, geometric and loading parameters of the coated system. Specifically, effects of interfacial cracking on the distributions of the contact pressure and the in-plane stress component along the coating surface are examined and the mixed-mode stress intensity factors evaluated from the crack-tip stress field with the square-root singularity are provided as a function of punch location. Further addressed is the quantification of the singular character of contact pressure distributions at the trailing and leading edges of the flat punch in terms of the punch-edge stress intensity factors. Implicit in this particular analysis of the coupled crack/contact problem presented henceforth is that the crack closure behaviour under the compressive contact stress field is not taken into account, ignoring the influence of crack-face contact and friction.

Keywords: interface crack; flat punch; coating/substrate system; functionally graded materials; contact mechanics; fracture mechanics

*Author for correspondence (hjchoi@kookmin.ac.kr).

Electronic supplementary material is available at <http://dx.doi.org/10.1098/rspa.2009.0437> or via <http://rspa.royalsocietypublishing.org>.

1. Introduction

Coating/substrate systems are commonly utilized in a wide range of modern engineering practices, in an effort to improve the reliability and durability of components and parts of mechanical and structural assemblages, where the coating materials are essentially intended to play a protective role for the underlying substrate against detrimental wear-, heat- and corrosion-related damage. In applying a conventional, homogeneous coating to the substrate, one of the issues of utmost significance is the unavoidable presence of a sharp interface with an apparent mismatch of thermophysical properties. It is therefore very likely that the interfacial region suffers from high stress concentrations, poor bonding strength and consequent vulnerability to failures that may involve cracking and debonding of the coating layer, thereby counteracting the enhancements attained by the coating. Recent progress in the field of functionally graded materials that exhibit smooth spatial variations of properties, however, has made it viable to cope with such a drawback through the deliberate incorporation of a graded transitional interlayer as an undercoat between the coating and the substrate or the direct deposit of a graded coating on the substrate as an alternative to the homogeneous coating. The mismatch between the properties of the constituents can thus be alleviated to such a degree that it leads to superior structural and tribological performances (Schulz *et al.* 2003).

On the premise that certain standard classes of boundary value problems are to be resolved in conjunction with the characterization of this new generation of engineered materials for many technologically important applications, a series of benchmark solutions to a variety of fracture and contact mechanics problems has been obtained for graded, non-homogeneous solids, as described by Erdogan & Ozturk (2008). When it comes to fracture mechanics analysis, the distinct problem area is the identification of crack-tip singularities with the aim of quantifying the effect of material gradations on crack driving forces and other fracture-related parameters. A thorough review of corresponding earlier studies of key interest was also given by Erdogan (1998), highlighting the salient features concerning the crack-tip behaviour that entails the graded properties. The most noteworthy is the near-tip field possessing square-root singularity along with the same angular distributions around the crack tip as those in the homogeneous material, provided the spatially varying elastic modulus is continuous and piecewise differentiable near and at the crack tip (see also Eischen 1987; Jin & Noda 1994). Hence, the effect of material gradients was shown to manifest itself through the values of crack-tip stress intensity factors. A number of additional contributions in the quasi-static crack problems were reported, among others, by Choi (2001*a*, 2007*a*), Paulino *et al.* (2003) and Chan *et al.* (2008), while those addressing the elastodynamic response to impact loading are due to Choi (2004, 2006, 2007*b*), Lee & Choi (2006) and Song & Paulino (2006). In addition, the crack problems involving the thermoelastically graded properties were dealt with by Lee & Erdogan (1998), Choi (2003), Walters *et al.* (2004) and Dag (2006).

From the standpoint of contact mechanics that could find applications where surface wear and damage due to sliding contact are a serious concern, such as in the design of load transfer components with property

gradations, some mechanistic and phenomenological observations were made by Suresh *et al.* (1997) and Jitcharoen *et al.* (1998). Specifically, when compared with the results of contact mechanics analysis in the homogeneous solid (Hills *et al.* 1993), the appropriate gradual variation of the elastic modulus was shown to significantly alter the stress field around the contact region. Further illustrated by Suresh (2001) was that the controlled gradients in the elastic properties offer unique opportunities for the design of surfaces with improved resistance to sliding-contact deformation and damage that cannot be realized in the conventional homogeneous material. It was Guler & Erdogan (2004) who examined the contact stress field for the graded coating bonded to a homogeneous substrate indented by frictional rigid punches with various profiles. The same problem but with arbitrary spatial variations of shear modulus was treated by Ke & Wang (2007), based on a multilayered approach. Moreover, Choi & Paulino (2008) considered the problem of thermoelastic contact mechanics for a flat punch sliding over the graded coating/substrate system with frictional heat generation.

In many engineering problems of practical interest, the mechanical and structural members are exposed to frequent occurrences of various cracking modes under the influence of a stress field imposed as a result of contact loading through indentation. Such situations have been the subject of increasing importance, requiring the development of appropriate analytical and numerical models in extending the fracture mechanics-based predictions to more complicated problems where severe stress gradients persist in the vicinity of contact loading. Typically these may involve the studies, for example, by Keer *et al.* (1982), Bryant *et al.* (1984), Hasebe *et al.* (1989), Bower & Fleck (1994) and Munisamy *et al.* (1995) for the contact fracture analyses of uncoated homogeneous solids and those by Oliveira & Bower (1996) and Zalounina & Andreasen (2004) for the cases of coated media having dissimilar homogeneous properties, with a diverse degree of sophistication. To be specific, Keer *et al.* (1982) and Bower & Fleck (1994) assumed that the elastic half-space is simply subjected to normal and shear loading that resembles the frictional Hertzian stresses, and Oliveira & Bower (1996) also employed the contact pressure distribution that remains Hertzian despite the mismatch in elastic properties across the interface between the coating and the substrate. On the other hand, Bryant *et al.* (1984) and Hasebe *et al.* (1989) presented the solutions to the problem of a crack loaded by a rigid punch passing along the surface of a homogeneous half-plane, taking the interaction between the crack and the contact into account. Munisamy *et al.* (1995) carried out the analysis to examine the effect of the crack-induced compliance change in a half-plane on the pressure distribution beneath a rigid flat indenter and on the crack-tip stress intensity factors as well, while Zalounina & Andreasen (2004) formulated a problem of frictionless rolling contact between an edge-cracked coated solid and a rigid circular indenter. In the light of a number of potential benefits achievable from the use of functionally graded materials, especially in the field of wear-resistant coatings, Choi (2001*b*) and El-Borgi *et al.* (2004) considered the problem of a crack in a graded coating/substrate system, where the cracked medium was assumed to be loaded solely by the applied Hertzian contact stresses, and Dag & Erdogan (2002) tackled the coupled problem for a semi-infinite graded medium containing a surface crack and loaded by a sliding rigid punch.

It can now be inferred that the attempts undertaken to date for contact fracture analyses involving the functionally graded materials are rather restrictive. The objective of this paper is, therefore, to investigate a coupled crack/contact problem of a coating/substrate system with graded properties, within the framework of plane elasticity. The graded material is assumed to exist as a non-homogeneous interlayer between dissimilar, homogeneous phases of the coated medium loaded on its surface by a frictional sliding flat punch, with a crack being located along the interface between the interlayer and the substrate. As the method of solution and analysis, the Fourier integral transform and the transfer matrix approach (Bahar 1972) are employed and a set of three simultaneous Cauchy-type singular integral equations is derived for the derivatives of crack-face displacements and the contact pressure. Numerical results are obtained to address the interactions between the contact stress field and the crack-tip behaviour for various combinations of material, geometric and loading parameters of the coated system. In particular, the effects of interfacial cracking on the distributions of the contact pressure and the in-plane stress along the coating surface are examined and the mixed-mode crack-tip stress intensity factors are provided as a function of punch location. Furthermore, with a view to quantifying the degree of criticality of the local intensification of singular stresses that build up at the edges of the flat punch, the punch-edge stress intensity factors are also defined and evaluated, in parallel with the concept used for characterizing the singular behaviour of crack-tip stresses.

2. Formulation of the coupled crack/contact problem

A schematic of the problem under consideration is depicted in figure 1, where a homogeneous coating layer is deposited on a substrate with a graded interlayer between. A rigid flat punch of width 2δ is pressed against the coating by a normal force P and slides in the positive y -direction, with a frictional shear force $Q = \mu_f P$ developed between the punch and the coating surface by Coulomb's friction, where μ_f is the coefficient of friction. The interface between the interlayer and the substrate is assumed to contain a crack of length $2c$, the centre of which is located at a distance e from that of the punch.

The coating, the interlayer and the substrate are distinguished in order from the top with the thickness h_j , $j = 1, 2$, and semi-infinite and the shear moduli μ_j , $j = 1, 2, 3$, respectively. The non-homogeneous shear modulus $\mu_2(x)$ of the graded interlayer is approximated in the form as (Erdogan 1998)

$$\mu_2(x) = \mu_1 e^{\beta x} \quad \text{and} \quad \beta = \frac{1}{h_2} \ln \left(\frac{\mu_3}{\mu_1} \right), \quad (2.1)$$

where the gradation parameter β specified in the local coordinates $(x, y) = (x_j, y)$, $j = 1, 2, 3$, satisfies the continuous transition of the shear moduli from the coating to the substrate and the spatial variation of Poisson's ratio is assumed to be negligible throughout the medium such that $\nu_j = \nu = \text{constant}$.

Let $u_j(x, y)$ and $v_j(x, y)$, $j = 1, 2, 3$, be the displacement components in the x - and y -directions, respectively, so that the Navier–Cauchy equations of

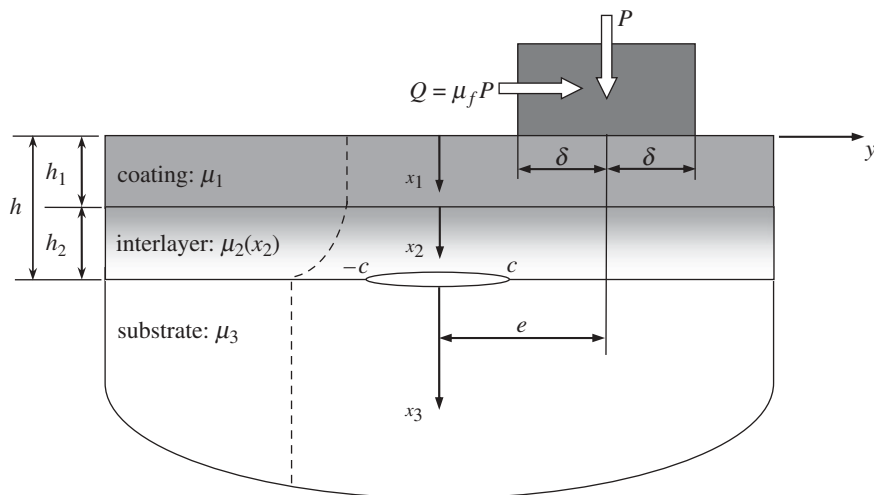


Figure 1. Schematic of the coupled crack/contact problem for a coating/substrate system with graded properties.

equilibrium in the absence of body forces are written as

$$\nabla^2 u_j + \frac{2}{\kappa - 1} \left(\frac{\partial^2 u_j}{\partial x^2} + \frac{\partial^2 v_j}{\partial x \partial y} \right) + \frac{\beta}{\kappa - 1} \left[(\kappa + 1) \frac{\partial u_j}{\partial x} + (3 - \kappa) \frac{\partial v_j}{\partial y} \right] = 0, \quad (2.2)$$

$$\nabla^2 v_j + \frac{2}{\kappa - 1} \left(\frac{\partial^2 v_j}{\partial y^2} + \frac{\partial^2 u_j}{\partial x \partial y} \right) + \beta \left(\frac{\partial v_j}{\partial x} + \frac{\partial u_j}{\partial y} \right) = 0, \quad j = 1, 2, 3, \quad (2.3)$$

where $\kappa = 3 - 4\nu$ for the plane strain and $\kappa = (3 - \nu)/(1 + \nu)$ for the plane stress, $\beta \neq 0$ for the graded interlayer ($j = 2$) and $\beta = 0$ for the homogeneous constituents ($j = 1, 3$), and the stress components $\sigma_{kij}(x, y)$, $k = 1, 2, 3$, $i, j = x, y$, are evaluated from the following constitutive relations:

$$\sigma_{jxx} = \frac{\mu_j}{\kappa - 1} \left[(\kappa + 1) \frac{\partial u_j}{\partial x} + (3 - \kappa) \frac{\partial v_j}{\partial y} \right], \quad (2.4)$$

$$\sigma_{jyy} = \frac{\mu_j}{\kappa - 1} \left[(\kappa + 1) \frac{\partial v_j}{\partial y} + (3 - \kappa) \frac{\partial u_j}{\partial x} \right], \quad (2.5)$$

$$\sigma_{jxy} = \mu_j \left(\frac{\partial u_j}{\partial y} + \frac{\partial v_j}{\partial x} \right), \quad j = 1, 2, 3. \quad (2.6)$$

A set of homogeneous boundary and interface conditions for the coupled problem is written in the local coordinates $(x, y) = (x_j, y)$, $j = 1, 2, 3$, such that

$$u_1(h_1, y) = u_2(0, y), \quad v_1(h_1, y) = v_2(0, y), \quad |y| < \infty, \quad (2.7)$$

$$\sigma_{jxx}(h_j, y) = \sigma_{(j+1)xx}(0, y), \quad \sigma_{jxy}(h_j, y) = \sigma_{(j+1)xy}(0, y), \quad j = 1, 2, |y| < \infty, \quad (2.8)$$

$$u_3(\infty, y) = 0, \quad v_3(\infty, y) = 0, \quad |y| < \infty, \quad (2.9)$$

and the mixed conditions along the cracked interface are imposed as

$$u_2(h_2, y) = u_3(0, y), \quad v_2(h_2, y) = v_3(0, y), \quad |y| > c, \quad (2.10)$$

$$\sigma_{3xx}(0, y) = 0, \quad \sigma_{3xy}(0, y) = 0, \quad |y| < c, \quad (2.11)$$

while those along the surface of the coating in contact with the frictional punch are expressed as

$$u_1(0, y) = f(y), \quad \sigma_{1xy}(0, y) = \mu_f \sigma_{1xx}(0, y), \quad |y - e| < \delta, \quad (2.12)$$

$$\sigma_{1xx}(0, y) = 0, \quad \sigma_{1xy}(0, y) = 0, \quad |y - e| > \delta, \quad (2.13)$$

where $f(y)$ refers to the indentation deformation at the coating surface presumed *a priori* to be within the contact area via the prescribed punch profile.

In order to account for disturbances caused by the presence of interfacial cracking as well as by the action of the punch, the unknown auxiliary functions are defined as

$$\phi_1(y) = \frac{\partial}{\partial y} [u_3(0, y) - u_2(h_2, y)], \quad |y| < c, \quad (2.14)$$

$$\phi_2(y) = \frac{\partial}{\partial y} [v_3(0, y) - v_2(h_2, y)], \quad |y| < c, \quad (2.15)$$

$$\phi_3(y) = -\sigma_{1xx}(0, y), \quad |y - e| < \delta, \quad (2.16)$$

under the condition of single valuedness of displacements along the cracked interface and that of overall equilibrium with the resultant contact force P such that

$$\int_{-c}^c \phi_j(y) dy = 0, \quad j = 1, 2 \quad \text{and} \quad \int_{e-\delta}^{e+\delta} \phi_3(y) dy = P. \quad (2.17)$$

The general solutions for the displacements in the coating layer ($\beta = 0$ and $(x, y) = (x_1, y)$) are obtained by solving the governing equations (2.2) and (2.3) based on the Fourier integral transform method as

$$u_1(x, y) = \frac{i}{2\pi} \int_{-\infty}^{\infty} \left\{ \left[F_{11} + F_{12} \left(x - \frac{\kappa}{s} \right) \right] e^{sx} - \left[F_{13} + F_{14} \left(x + \frac{\kappa}{s} \right) \right] e^{-sx} \right\} e^{-isy} ds, \quad (2.18)$$

$$v_1(x, y) = \frac{1}{2\pi} \int_{-\infty}^{\infty} \left[(F_{11} + F_{12}x) e^{sx} + (F_{13} + F_{14}x) e^{-sx} \right] e^{-isy} ds, \quad 0 \leq x \leq h_1, \quad (2.19)$$

where s is the transform variable, $i = (-1)^{1/2}$, and $F_{1j}(s)$, $j = 1, \dots, 4$, are arbitrary unknowns.

For the graded, non-homogeneous interlayer ($\beta \neq 0$ and $(x, y) = (x_2, y)$), the general expressions of the displacement components can be obtained as

$$u_2(x, y) = -\frac{i}{2\pi} \int_{-\infty}^{\infty} \sum_{j=1}^4 F_{2j} m_j e^{n_j x - i s y} ds, \quad (2.20)$$

$$v_2(x, y) = \frac{1}{2\pi} \int_{-\infty}^{\infty} \sum_{j=1}^4 F_{2j} e^{n_j x - i s y} ds, \quad 0 \leq x \leq h_2, \quad (2.21)$$

where $F_{2j}(s)$, $j = 1, \dots, 4$, are arbitrary unknowns, $n_j(s)$, $j = 1, \dots, 4$, are the roots of the characteristic equation

$$(n^2 + \beta n - s^2)^2 + \left(\frac{3 - \kappa}{1 + \kappa}\right) \beta^2 s^2 = 0, \quad (2.22)$$

from which it follows that

$$n_j = -\frac{\beta}{2} + \sqrt{\frac{\beta^2}{4} + s^2 - i(-1)^j \beta s \left(\frac{3 - \kappa}{1 + \kappa}\right)^{1/2}}; \quad \text{Re}(n_j) > 0, \quad j = 1, 2, \quad (2.23)$$

$$n_j = -\frac{\beta}{2} - \sqrt{\frac{\beta^2}{4} + s^2 + i(-1)^j \beta s \left(\frac{3 - \kappa}{1 + \kappa}\right)^{1/2}}; \quad \text{Re}(n_j) < 0, \quad j = 3, 4, \quad (2.24)$$

and $m_j(s)$, $j = 1, \dots, 4$, are given for each root $n_j(s)$, $j = 1, \dots, 4$, as

$$m_j = \frac{(\kappa - 1)(n_j^2 + \beta n_j) - (\kappa + 1)s^2}{[2n_j + (\kappa - 1)\beta]s}. \quad (2.25)$$

The general solutions for the displacements in the semi-infinite, homogeneous substrate ($\beta = 0$ and $(x, y) = (x_3, y)$) that fulfils the regularity condition in equation (2.9) is also readily obtainable as

$$u_3(x, y) = -\frac{i}{2\pi} \int_{-\infty}^{\infty} \frac{s}{|s|} \left[F_{31} + F_{32} \left(x + \frac{\kappa}{|s|} \right) \right] e^{-|s|x - i s y} ds, \quad (2.26)$$

$$v_3(x, y) = \frac{1}{2\pi} \int_{-\infty}^{\infty} (F_{31} + F_{32} x) e^{-|s|x - i s y} ds; \quad 0 \leq x < \infty, \quad (2.27)$$

where $F_{3j}(s)$, $j = 1, 2$, are arbitrary unknowns.

The next step in the solution procedure requires the components of displacements and stresses in the constituents be determined in terms of the auxiliary functions ϕ_j , $j = 1, 2, 3$. In the coupled crack/contact problem at hand, this is made in two parts: (1) the interface crack problem for the coated system with a traction-free boundary where the displacements and stresses are obtained in terms of ϕ_1 and ϕ_2 in equations (2.14) and (2.15), with ϕ_3 being zero, and (2) the contact problem without a crack where the corresponding components are expressed solely in terms of ϕ_3 in equation (2.16). As a result, the total displacement and stress fields throughout the cracked medium loaded by the

punch are represented as the sum of those obtained for each problem as

$$u_j(x, y) = u_j^{(1)}(x, y) + u_j^{(2)}(x, y), \quad j = 1, 2, 3, \quad (2.28)$$

$$v_j(x, y) = v_j^{(1)}(x, y) + v_j^{(2)}(x, y), \quad j = 1, 2, 3, \quad (2.29)$$

$$\sigma_{jkl}(x, y) = \sigma_{jkl}^{(1)}(x, y) + \sigma_{jkl}^{(2)}(x, y), \quad j = 1, 2, 3, \quad k, l = x, y, \quad (2.30)$$

which should thus satisfy the crack-face and contact boundary conditions of the original coupled problem, equations (2.11) and (2.12), simultaneously, where the superscript (1)/(2) stands for the problem (1)/(2).

3. Transfer matrix approach for the crack and contact problems

For the three-layer coating/substrate system, the general solutions of plane elasticity equations involve a total of 10 unknowns, $F_{ij}(s)$, $i = 1, 2, j = 1, \dots, 4$, and $F_{3j}(s)$, $j = 1, 2$, in each part of the formulation. As mentioned above, these unknowns should be obtained in terms of ϕ_1 and ϕ_2 for the crack problem and in terms of ϕ_3 for the contact problem from the two separate sets of relevant boundary and interface conditions. As a judicious way of circumventing the complexities that may arise from such lengthy algebraic manipulations, the transfer matrix approach (Bahar 1972) is extended to the current analysis of the coupled crack/contact problem. The auxiliary functions ϕ_j , $j = 1, 2, 3$, then become the only unknowns that remain to be evaluated from the crack-face and contact boundary conditions.

(a) The crack problem—1

From the general solutions in equations (2.18)–(2.27) and the constitutive equations (2.4)–(2.6), the displacements and tractions in the coated system are written in the Fourier-transformed domain as

$$\mathbf{f}_j(x, s) = \mathbf{T}_j(x, s)\mathbf{a}_j(s), \quad j = 1, 2, 3, \quad (3.1)$$

where $\mathbf{f}_j(x, s)$, $j = 1, 2, 3$, are state vectors containing the physical quantities in each of the constituents, $\mathbf{a}_j(s)$, $j = 1, 2, 3$, are vectors for the arbitrary unknowns in the general solutions of elasticity equations such that

$$\mathbf{f}_j(x, s) = \{ \bar{u}_j(x, s)/i, \quad \bar{v}_j(x, s), \quad \bar{\sigma}_{jxx}(x, s)/i, \quad \bar{\sigma}_{jxy}(x, s) \}^T, \quad j = 1, 2, 3, \quad (3.2)$$

$$\mathbf{a}_j(s) = \{ F_{j1}(s), F_{j2}(s), F_{j3}(s), F_{j4}(s) \}^T, \quad j = 1, 2, \quad (3.3)$$

$$\mathbf{a}_3(s) = \{ F_{31}(s), F_{32}(s) \}^T, \quad (3.4)$$

and $\mathbf{T}_j(x, s)$, $j = 1, 2, 3$, are matrices which are a function of the elastic parameters of the constituents as well as the variables x and s , and 4×4 for the coating and the interlayer ($j = 1, 2$) and 4×2 for the substrate ($j = 3$).

In terms of the state vector equations, the boundary and interface conditions for the crack problem can be expressed as

$$\mathbf{T}_1^-(s)\mathbf{a}_1(s) = \mathbf{f}_{01}(s) = \{\bar{u}_1^-(s)/i, \bar{v}_1^-(s), 0, 0\}^T, \quad (3.5)$$

$$\mathbf{T}_1^+(s)\mathbf{a}_1(s) = \mathbf{T}_2^-(s)\mathbf{a}_2(s), \quad (3.6)$$

$$\mathbf{T}_2^+(s)\mathbf{a}_2(s) - \mathbf{T}_3^-(s)\mathbf{a}_3(s) = \Delta\bar{\mathbf{u}}_0(s), \quad (3.7)$$

where the superscript $-/+$ denotes the upper/lower surface of the constituents and $\Delta\bar{\mathbf{u}}_0(s)$ is a vector of length 4 containing the Fourier transforms of the auxiliary functions ϕ_j , $j=1, 2$, and the zero elements

$$\Delta\bar{\mathbf{u}}_0(s) = \{-\Delta\bar{u}(s)/i, -\Delta\bar{v}(s), 0, 0\}^T, \quad (3.8)$$

$$\Delta\bar{u}(s) = \frac{i}{s} \int_{-c}^c \phi_1(r) e^{isr} dr, \quad \Delta\bar{v}(s) = \frac{i}{s} \int_{-c}^c \phi_2(r) e^{isr} dr. \quad (3.9)$$

Successive eliminations of the unknown vectors, $\mathbf{a}_j(s)$, $j=1, 2$, from equations (3.5)–(3.7) allow the surface values of the field quantities, $\mathbf{f}_{01}(s)$, in equation (3.5) to be written in terms of the unknown vectors $\mathbf{a}_3(s)$ and $\Delta\bar{\mathbf{u}}_0(s)$ as

$$\mathbf{G}_1(s)\mathbf{a}_3(s) + \mathbf{G}_2(s)\Delta\bar{\mathbf{u}}_0(s) = \mathbf{f}_{01}(s), \quad (3.10)$$

where $\mathbf{G}_1(s)$ is a 4×2 transfer matrix between the substrate and the upper surface of the coating and $\mathbf{G}_2(s)$ is a 4×4 transfer matrix between the cracked interface and the upper surface of the coating

$$\mathbf{G}_1(s) = \prod_{j=1}^3 \mathbf{H}_j(s), \quad \mathbf{G}_2(s) = \prod_{j=1}^2 \mathbf{H}_j(s), \quad (3.11)$$

in which the matrix functions, $\mathbf{H}_j(s)$, $j=1, 2, 3$, are defined by

$$\mathbf{H}_j(s) = \mathbf{T}_j^-(s) \left[\mathbf{T}_j^+(s) \right]^{-1}, \quad j=1, 2, \quad \mathbf{H}_3(s) = \mathbf{T}_3^-(s). \quad (3.12)$$

The transfer matrix equation (3.10) can be decomposed and solved for the vector $\mathbf{a}_3(s)$ and for the transformed surface displacements, $\bar{u}_1^-(s)$ and $\bar{v}_1^-(s)$ in equation (3.5), directly in terms of $\Delta\bar{\mathbf{u}}_0(s)$. After substituting the elements of $\mathbf{a}_3(s)$ into the state vector equation (3.1) for the substrate and using the expressions for $\bar{u}_1^-(s)$ and $\bar{v}_1^-(s)$, followed by the inverse Fourier transform, it can be shown that the traction components along the cracked interface and the displacement gradients on the upper surface of the coating induced by the presence of the crack are obtained in terms of ϕ_j , $j=1, 2$, such that

$$\sigma_{3xx}^{(1)}(0, y) = \int_{-c}^c \sum_{j=1}^2 M_{1j}^{(1)}(y, r) \phi_j(r) dr, \quad |y| < \infty, \quad (3.13)$$

$$\sigma_{3xy}^{(1)}(0, y) = \int_{-c}^c \sum_{j=1}^2 M_{2j}^{(1)}(y, r) \phi_j(r) dr, \quad |y| < \infty, \quad (3.14)$$

$$\frac{\partial u_1^{(1)}}{\partial y}(0, y) = \int_{-c}^c \sum_{j=1}^2 M_{3j}^{(1)}(y, r) \phi_j(r) \, dr, \quad |y| < \infty, \quad (3.15)$$

$$\frac{\partial v_1^{(1)}}{\partial y}(0, y) = \int_{-c}^c \sum_{j=1}^2 M_{4j}^{(1)}(y, r) \phi_j(r) \, dr, \quad |y| < \infty, \quad (3.16)$$

in which the kernel functions, $M_{ij}^{(1)}(s)$, $i = 1, 2, 3, 4$, $j = 1, 2$, are written as

$$\begin{aligned} M_{11}^{(1)}(y, r) &= -\frac{i}{2\pi} \int_{-\infty}^{\infty} \frac{1}{s} Q_{31}(s) e^{is(r-y)} \, ds, \\ M_{12}^{(1)}(y, r) &= \frac{1}{2\pi} \int_{-\infty}^{\infty} \frac{1}{s} Q_{32}(s) e^{is(r-y)} \, ds, \end{aligned} \quad (3.17)$$

$$\begin{aligned} M_{21}^{(1)}(y, r) &= -\frac{1}{2\pi} \int_{-\infty}^{\infty} \frac{1}{s} Q_{41}(s) e^{is(r-y)} \, ds, \\ M_{22}^{(1)}(y, r) &= -\frac{i}{2\pi} \int_{-\infty}^{\infty} \frac{1}{s} Q_{42}(s) e^{is(r-y)} \, ds, \end{aligned} \quad (3.18)$$

$$\begin{aligned} M_{31}^{(1)}(y, r) &= -\frac{1}{2\pi} \int_{-\infty}^{\infty} P_{11}(s) e^{is(r-y)} \, ds, \\ M_{32}^{(1)}(y, r) &= -\frac{i}{2\pi} \int_{-\infty}^{\infty} P_{12}(s) e^{is(r-y)} \, ds, \end{aligned} \quad (3.19)$$

$$\begin{aligned} M_{41}^{(1)}(y, r) &= \frac{i}{2\pi} \int_{-\infty}^{\infty} P_{21}(s) e^{is(r-y)} \, ds, \\ M_{42}^{(1)}(y, r) &= -\frac{1}{2\pi} \int_{-\infty}^{\infty} P_{22}(s) e^{is(r-y)} \, ds, \end{aligned} \quad (3.20)$$

where $Q_{ij}(s)$, $i = 3, 4$, $j = 1, 2$, and $P_{ij}(s)$, $i, j = 1, 2$, are, respectively, elements of the 4×2 and 2×2 matrices

$$\mathbf{Q}(s) = -\mathbf{T}_3^-(s) \begin{bmatrix} G_{31}^1 & G_{32}^1 \\ G_{41}^1 & G_{42}^1 \end{bmatrix}^{-1} \begin{bmatrix} G_{31}^2 & G_{32}^2 \\ G_{41}^2 & G_{42}^2 \end{bmatrix}, \quad (3.21)$$

$$\mathbf{P}(s) = \begin{bmatrix} G_{11}^2 & G_{12}^2 \\ G_{21}^2 & G_{22}^2 \end{bmatrix} - \begin{bmatrix} G_{11}^1 & G_{12}^1 \\ G_{21}^1 & G_{22}^1 \end{bmatrix} \begin{bmatrix} G_{31}^1 & G_{32}^1 \\ G_{41}^1 & G_{42}^1 \end{bmatrix}^{-1} \begin{bmatrix} G_{31}^2 & G_{32}^2 \\ G_{41}^2 & G_{42}^2 \end{bmatrix}, \quad (3.22)$$

in which the superscripts 1 and 2 in the right-hand side signify the elements of the transfer matrices $\mathbf{G}_1(s)$ and $\mathbf{G}_2(s)$, respectively, together with the following

asymptotic behaviour as $|s|$ approaches infinity:

$$\lim_{|s| \rightarrow \infty} \frac{1}{s} Q_{31}(s) = Q_{\infty} \left(\frac{|s|}{s} - \frac{\beta}{2s} \right) = \frac{2\mu_3}{\kappa + 1} \left(\frac{|s|}{s} - \frac{\beta}{2s} \right), \quad (3.23)$$

$$\lim_{|s| \rightarrow \infty} \frac{1}{s} Q_{42}(s) = Q_{\infty} \left(\frac{|s|}{s} - \frac{\beta}{4s} \right) = \frac{2\mu_3}{\kappa + 1} \left(\frac{|s|}{s} - \frac{\beta}{4s} \right), \quad (3.24)$$

$$\lim_{|s| \rightarrow \infty} \frac{1}{s} Q_{32}(s) = \lim_{|s| \rightarrow \infty} \frac{1}{s} Q_{41}(s) = Q_{\infty} \frac{\beta}{4|s|} = \frac{2\mu_3}{\kappa + 1} \frac{\beta}{4|s|}, \quad (3.25)$$

$$\lim_{|s| \rightarrow \infty} P_{ij}(s) = 0, \quad i, j = 1, 2. \quad (3.26)$$

(b) *The contact problem—2*

For the contact problem, the corresponding boundary and interface conditions are also expressed in terms of the state vector equations as

$$\mathbf{T}_1^-(s) \mathbf{a}_1(s) = \mathbf{f}_{02}(s) = \{\bar{u}_1^-(s)/i, \bar{v}_1^-(s), \bar{\sigma}_o(s)/i, \bar{\tau}_o(s)\}^T, \quad (3.27)$$

$$\mathbf{T}_1^+(s) \mathbf{a}_1(s) = \mathbf{T}_2^-(s) \mathbf{a}_2(s), \quad (3.28)$$

$$\mathbf{T}_2^+(s) \mathbf{a}_2(s) = \mathbf{T}_3^-(s) \mathbf{a}_3(s), \quad (3.29)$$

where $\bar{\sigma}_o(s)$ and $\bar{\tau}_o(s)$ are the transformed normal and tangential tractions acting on the upper surface of the coating such that

$$\bar{\sigma}_o(s) = - \int_{e^{-\delta}}^{e^{+\delta}} \phi_3(r) e^{isr} dr, \quad \bar{\tau}_o(s) = -\mu_f \int_{e^{-\delta}}^{e^{+\delta}} \phi_3(r) e^{isr} dr, \quad (3.30)$$

and upon removing the unknown vectors, $\mathbf{a}_j(s)$, $j = 1, 2$, from equations (3.27)–(3.29), the surface values of the field quantities, $\mathbf{f}_{02}(s)$, in equation (3.27) can be written in terms of the unknown vector $\mathbf{a}_3(s)$ as

$$\mathbf{G}_1(s) \mathbf{a}_3(s) = \mathbf{f}_{02}(s), \quad (3.31)$$

in which $\mathbf{G}_1(s)$ is the 4×2 transfer matrix defined in equation (3.11).

Likewise, the above transfer matrix equation is solved for the vector $\mathbf{a}_3(s)$ in terms of the transformed tractions, $\bar{\sigma}_o(s)$ and $\bar{\tau}_o(s)$, to be substituted into the state vector equation (3.1) for the substrate. The transformed surface displacements, $\bar{u}_1^-(s)$ and $\bar{v}_1^-(s)$, are also obtainable in terms of $\bar{\sigma}_o(s)$ and $\bar{\tau}_o(s)$. After taking the inverse Fourier transform, the traction components along the nominal interface between the interlayer and the substrate and the displacement gradients on the upper surface of the coating due to the action of the frictional punch can be expressed in terms of ϕ_3 as

$$\sigma_{3xx}^{(2)}(0, y) = \int_{e^{-\delta}}^{e^{+\delta}} \left[M_{11}^{(2)}(y, r) + \mu_f M_{12}^{(2)}(y, r) \right] \phi_3(r) dr, \quad |y| < \infty, \quad (3.32)$$

$$\sigma_{3xy}^{(2)}(0, y) = \int_{e^{-\delta}}^{e^{+\delta}} \left[M_{21}^{(2)}(y, r) + \mu_f M_{22}^{(2)}(y, r) \right] \phi_3(r) dr, \quad |y| < \infty, \quad (3.33)$$

$$\frac{\partial u_1^{(2)}}{\partial y}(0, y) = \int_{\epsilon-\delta}^{\epsilon+\delta} \left[M_{31}^{(2)}(y, r) + \mu_f M_{32}^{(2)}(y, r) \right] \phi_3(r) dr, \quad |y| < \infty, \quad (3.34)$$

$$\frac{\partial v_1^{(2)}}{\partial y}(0, y) = \int_{\epsilon-\delta}^{\epsilon+\delta} \left[M_{41}^{(2)}(y, r) + \mu_f M_{42}^{(2)}(y, r) \right] \phi_3(r) dr, \quad |y| < \infty, \quad (3.35)$$

together with the kernel functions, $M_{ij}^{(2)}(s)$, $i = 1, 2, 3, 4$, $j = 1, 2$, given by

$$M_{11}^{(2)}(y, r) = -\frac{1}{2\pi} \int_{-\infty}^{\infty} L_{31}(s) e^{is(r-y)} ds, \quad M_{12}^{(2)}(y, r) = -\frac{i}{2\pi} \int_{-\infty}^{\infty} L_{32}(s) e^{is(r-y)} ds, \quad (3.36)$$

$$M_{21}^{(2)}(y, r) = \frac{i}{2\pi} \int_{-\infty}^{\infty} L_{41}(s) e^{is(r-y)} ds, \quad M_{22}^{(2)}(y, r) = -\frac{1}{2\pi} \int_{-\infty}^{\infty} L_{42}(s) e^{is(r-y)} ds, \quad (3.37)$$

$$M_{31}^{(2)}(y, r) = \frac{i}{2\pi} \int_{-\infty}^{\infty} s N_{11}(s) e^{is(r-y)} ds, \quad M_{32}^{(2)}(y, r) = -\frac{1}{2\pi} \int_{-\infty}^{\infty} s N_{12}(s) e^{is(r-y)} ds, \quad (3.38)$$

$$M_{41}^{(2)}(y, r) = \frac{1}{2\pi} \int_{-\infty}^{\infty} s N_{21}(s) e^{is(r-y)} ds, \quad M_{42}^{(2)}(y, r) = \frac{i}{2\pi} \int_{-\infty}^{\infty} s N_{22}(s) e^{is(r-y)} ds, \quad (3.39)$$

where $L_{ij}(s)$, $i = 3, 4$, $j = 1, 2$, are elements of the 4×2 matrix and $N_{ij}(s)$, $i, j = 1, 2$, are those of the 2×2 matrix as

$$\mathbf{L}(s) = \mathbf{T}_3^{-1}(s) \begin{bmatrix} G_{31}^1 & G_{32}^1 \\ G_{41}^1 & G_{42}^1 \end{bmatrix}^{-1}, \quad \mathbf{N}(s) = \begin{bmatrix} G_{11}^1 & G_{12}^1 \\ G_{21}^1 & G_{22}^1 \end{bmatrix} \begin{bmatrix} G_{31}^1 & G_{32}^1 \\ G_{41}^1 & G_{42}^1 \end{bmatrix}^{-1}, \quad (3.40)$$

which possess the following asymptotic trends for the large values of $|s|$:

$$\lim_{|s| \rightarrow \infty} L_{ij}(s) = 0, \quad i = 3, 4, \quad j = 1, 2, \quad (3.41)$$

$$\lim_{|s| \rightarrow \infty} s N_{11}(s) = \lim_{|s| \rightarrow \infty} s N_{22}(s) = N_1^\infty \frac{|s|}{s} = -\frac{\kappa + 1}{4\mu_1} \frac{|s|}{s}, \quad (3.42)$$

$$\lim_{|s| \rightarrow \infty} s N_{12}(s) = \lim_{|s| \rightarrow \infty} s N_{21}(s) = N_2^\infty = -\frac{\kappa - 1}{4\mu_1}. \quad (3.43)$$

4. Integral equations for the coupled crack/contact problem

In the coupled crack/contact problem under consideration, by superimposing the relevant expressions, the tractions along the cracked interface are written in terms of the auxiliary functions ϕ_j , $j = 1, 2, 3$, as

$$\begin{aligned} \sigma_{3xx}(0, y) = & \int_{-c}^c \sum_{j=1}^2 M_{1j}^{(1)}(y, r) \phi_j(r) dr \\ & + \int_{e-\delta}^{e+\delta} \left[M_{11}^{(2)}(y, r) + \mu_f M_{12}^{(2)}(y, r) \right] \phi_3(r) dr, \quad |y| < \infty, \end{aligned} \quad (4.1)$$

$$\begin{aligned} \sigma_{3xy}(0, y) = & \int_{-c}^c \sum_{j=1}^2 M_{2j}^{(1)}(y, r) \phi_j(r) dr \\ & + \int_{e-\delta}^{e+\delta} \left[M_{21}^{(2)}(y, r) + \mu_f M_{22}^{(2)}(y, r) \right] \phi_3(r) dr, \quad |y| < \infty, \end{aligned} \quad (4.2)$$

and the displacement gradients on the coating surface are also obtained in terms of ϕ_j , $j = 1, 2, 3$, such that

$$\begin{aligned} \frac{\partial u_1}{\partial y}(0, y) = & \int_{-c}^c \sum_{j=1}^2 M_{3j}^{(1)}(y, r) \phi_j(r) dr \\ & + \int_{e-\delta}^{e+\delta} \left[M_{31}^{(2)}(y, r) + \mu_f M_{32}^{(2)}(y, r) \right] \phi_3(r) dr, \quad |y| < \infty, \end{aligned} \quad (4.3)$$

$$\begin{aligned} \frac{\partial v_1}{\partial y}(0, y) = & \int_{-c}^c \sum_{j=1}^2 M_{4j}^{(1)}(y, r) \phi_j(r) dr \\ & + \int_{e-\delta}^{e+\delta} \left[M_{41}^{(2)}(y, r) + \mu_f M_{42}^{(2)}(y, r) \right] \phi_3(r) dr, \quad |y| < \infty. \end{aligned} \quad (4.4)$$

Subsequently, after separating the leading terms as identified in equations (3.23)–(3.25), (3.42) and (3.43) from the kernels in equations (4.1)–(4.4), followed by the use of Fourier representation of generalized functions given by (Friedman 1991)

$$\int_0^\infty \sin s(r-y) ds = \frac{1}{r-y}, \quad \int_0^\infty \cos s(r-y) ds = \pi \delta(r-y), \quad (4.5)$$

$$\int_0^\infty \frac{1}{s} \cos s(r-y) ds = -\ln|r-y|, \quad \int_0^\infty \frac{1}{s} \sin s(r-y) ds = \frac{\pi}{2} \operatorname{sgn}(r-y), \quad (4.6)$$

where $\delta(r-y)$ is the Dirac delta function, and applying the remaining conditions of traction-free crack faces in equation (2.11) and zero surface slope of the flat punch within the contact area via equation (2.12), i.e. $f(y) = \text{constant}$, one can

obtain a set of three simultaneous Cauchy-type singular integral equations as

$$\begin{aligned} & \frac{1}{\pi} \frac{2\mu_3}{\kappa + 1} \int_{-c}^c \frac{\phi_1(r)}{r - y} dr + \int_{-c}^c \sum_{j=1}^2 k_{1j}(y, r) \phi_j(r) dr \\ & + \int_{e-\delta}^{e+\delta} [g_{11}(y, r) + \mu_f g_{12}(y, r)] \phi_3(r) dr = 0, \quad |y| < c, \end{aligned} \quad (4.7)$$

$$\begin{aligned} & \frac{1}{\pi} \frac{2\mu_3}{\kappa + 1} \int_{-c}^c \frac{\phi_2(r)}{r - y} dr + \int_{-c}^c \sum_{j=1}^2 k_{2j}(y, r) \phi_j(r) dr \\ & + \int_{e-\delta}^{e+\delta} [g_{21}(y, r) + \mu_f g_{22}(y, r)] \phi_3(r) dr = 0, \quad |y| < c, \end{aligned} \quad (4.8)$$

$$\begin{aligned} & \mu_f \frac{\kappa - 1}{4\mu_1} \phi_3(y) + \frac{1}{\pi} \frac{\kappa + 1}{4\mu_1} \int_{e-\delta}^{e+\delta} \frac{\phi_3(r)}{r - y} dr + \int_{e-\delta}^{e+\delta} [k_{31}(y, r) + \mu_f k_{32}(y, r)] \phi_3(r) dr \\ & + \int_{-c}^c \sum_{j=1}^2 g_{3j}(y, r) \phi_j(r) dr = 0, \quad |y - e| < \delta, \end{aligned} \quad (4.9)$$

subjected to the satisfaction of compatibility and equilibrium conditions in equation (2.17), where the kernels, $k_{ij}(y, r)$ and $g_{ij}(y, r)$, $i=1, 2, 3$, $j=1, 2$, are expressed as

$$k_{11}(y, r) = \frac{1}{\pi} \int_0^\infty \left[\frac{1}{s} Q_{31}(s) - Q_\infty \left(1 - \frac{\beta}{2s} \right) \right] \sin s(r - y) ds - \frac{\beta Q_\infty}{4} \operatorname{sgn}(r - y), \quad (4.10)$$

$$k_{12}(y, r) = \frac{1}{\pi} \int_0^\infty \left[\frac{1}{s} Q_{32}(s) - \frac{Q_\infty \beta}{4s} \right] \cos s(r - y) ds - \frac{Q_\infty \beta}{4\pi} \ln |r - y|, \quad (4.11)$$

$$k_{21}(y, r) = -\frac{1}{\pi} \int_0^\infty \left[\frac{1}{s} Q_{41}(s) - \frac{Q_\infty \beta}{4s} \right] \cos s(r - y) ds + \frac{Q_\infty \beta}{4\pi} \ln |r - y|, \quad (4.12)$$

$$k_{22}(y, r) = \frac{1}{\pi} \int_0^\infty \left[\frac{1}{s} Q_{42}(s) - Q_\infty \left(1 - \frac{\beta}{4s} \right) \right] \sin s(r - y) ds - \frac{\beta Q_\infty}{8} \operatorname{sgn}(r - y), \quad (4.13)$$

$$k_{31}(y, r) = -\frac{1}{\pi} \int_0^\infty [s N_{11}(s) - N_1^\infty] \sin s(r - y) ds, \quad (4.14)$$

$$k_{32}(y, r) = -\frac{1}{\pi} \int_0^\infty [s N_{12}(s) - N_2^\infty] \cos s(r - y) ds, \quad (4.15)$$

$$g_{11}(y, r) = -\frac{1}{\pi} \int_0^\infty L_{31}(s) \cos s(r - y) ds, \quad (4.16)$$

$$g_{12}(y, r) = \frac{1}{\pi} \int_0^\infty L_{32}(s) \sin s(r - y) ds, \quad (4.17)$$

$$g_{21}(y, r) = -\frac{1}{\pi} \int_0^{\infty} L_{41}(s) \sin s(r - y) \, ds, \quad (4.18)$$

$$g_{22}(y, r) = -\frac{1}{\pi} \int_0^{\infty} L_{42}(s) \cos s(r - y) \, ds, \quad (4.19)$$

$$g_{31}(y, r) = -\frac{1}{\pi} \int_0^{\infty} P_{11}(s) \cos s(r - y) \, ds, \quad (4.20)$$

$$g_{32}(y, r) = \frac{1}{\pi} \int_0^{\infty} P_{12}(s) \sin s(r - y) \, ds, \quad (4.21)$$

which are bounded for all values of r and y in the given intervals, except for the existence of logarithmic singularities in equations (4.11) and (4.12). These unbounded terms, however, can be treated as part of regular kernels in the presence of Cauchy singular kernels, $1/(r - y)$, in the sense that such logarithmic terms are square integrable without affecting the near-tip singular field (Erdogan 1998).

5. Solution procedure and stress intensity factors

Because the dominant singular kernels in equations (4.7)–(4.9) are attributable solely to the Cauchy type and the variations of shear moduli are continuous throughout the coated system, the standard square-root singularity is retained at the interfacial crack tips, as compared with the anomalous oscillatory singularity encountered for the case of an interface crack in piecewise homogeneous bonded media (Rice 1988). On the other hand, the edges of the rigid flat punch are with the yet-to-be determined singular orders. As a result, the functions, ϕ_j , $j = 1, 2, 3$, can be written as (Muskhelishvili 1953)

$$\phi_j(r) = \frac{f_j(r)}{\sqrt{c^2 - r^2}}, \quad |r| < c, j = 1, 2, \quad (5.1)$$

$$\phi_3(r) = (\delta + e - r)^{\lambda} (\delta - e + r)^{\omega} f_3(r), \quad |r - e| < \delta, \quad (5.2)$$

where $f_j(y)$, $j = 1, 2, 3$, are unknown functions, but bounded and non-zero at the end points.

In the normalized intervals specified as

$$(r, y) = (c\eta, c\xi), \quad |r| < c, |y| < c, |\eta, \xi| < 1, \quad (5.3)$$

$$(r, y) = (e + \delta\eta, e + \delta\xi), \quad |r - e| < \delta, |y - e| < \delta, |\eta, \xi| < 1, \quad (5.4)$$

the fundamental functions of the dominant parts of the integral equations that characterize the singular nature at the crack tips and at the punch edges are, respectively, found to be the weight functions of Chebyshev polynomials of the first kind $T_n(\eta)$ and Jacobi polynomials $P_n^{(\lambda, \omega)}(\eta)$ (Gradshteyn & Ryzhik 1980). The solutions to the set of singular integral equations (4.7)–(4.9) can therefore

be expressed in the form of the following series expansions:

$$\phi_1(r) = \tilde{\phi}_1(\eta) = \frac{1}{\sqrt{1-\eta^2}} \sum_{n=0}^{\infty} a_n T_n(\eta), \quad |\eta| < 1, \quad (5.5)$$

$$\phi_2(r) = \tilde{\phi}_2(\eta) = \frac{1}{\sqrt{1-\eta^2}} \sum_{n=0}^{\infty} b_n T_n(\eta), \quad |\eta| < 1, \quad (5.6)$$

$$\phi_3(r) = \tilde{\phi}_3(\eta) = w(\eta) \sum_{n=0}^{\infty} c_n P_n^{(\chi, \omega)}(\eta), \quad w(\eta) = (1-\eta)^\chi (1+\eta)^\omega, \quad |\eta| < 1, \quad (5.7)$$

where a_n , b_n and c_n , $n \geq 0$, are unknown coefficients and the orthogonality for $T_n(\eta)$ can show that $a_0 = 0$ and $b_0 = 0$ satisfy the single valuedness in equation (2.17). In addition, the physics of the flat punch problem dictates that the values of χ and ω , as the powers of stress singularity at the leading ($y = e + \delta$) and trailing ($y = e - \delta$) edges of the punch, respectively, be negative and determined as (Hills *et al.* 1993)

$$\chi = \frac{\theta}{\pi}, \omega = -\frac{\theta}{\pi} - 1 \quad \text{and} \quad \tan \theta = -\frac{1}{\mu_f} \frac{\kappa + 1}{\kappa - 1}, \quad -1 < (\chi, \omega) < 0. \quad (5.8)$$

With the kernels in equations (4.10)–(4.21) rewritten in the normalized intervals as

$$k_{ij}(y, r) = \tilde{k}_{ij}(\xi, \eta) \quad \text{and} \quad g_{ij}(y, r) = \tilde{g}_{ij}(\xi, \eta), \quad i = 1, 2, 3, \quad j = 1, 2, \quad (5.9)$$

after substituting from equations (5.3)–(5.7) into the integral equations (4.7)–(4.9) and the equilibrium condition in equation (2.17), truncating the series with a finite number of terms at $n = N$, and regularizing the singular parts based on the properties of the Chebyshev and Jacobi polynomials (Gradshteyn & Ryzhik 1980), it can be shown that equations (4.7)–(4.9) and (2.17) become

$$\sum_{n=1}^N [a_n A_1 U_{n-1}(\xi) + a_n H_n^{11}(\xi) + b_n H_n^{12}(\xi)] + \sum_{n=0}^N c_n H_n^{13}(\xi) = 0, \quad (5.10)$$

$$\sum_{n=1}^N [b_n A_1 U_{n-1}(\xi) + a_n H_n^{21}(\xi) + b_n H_n^{22}(\xi)] + \sum_{n=0}^N c_n H_n^{23}(\xi) = 0, \quad (5.11)$$

$$\begin{aligned} \sum_{n=0}^N c_n \left[-\frac{A_2}{2 \sin \pi \chi} P_{n-1}^{(-\chi, -\omega)}(\xi) \right] + \sum_{n=1}^N [a_n H_n^{31}(\xi) + b_n H_n^{32}(\xi)] \\ + \sum_{n=0}^N c_n H_n^{33}(\xi) = 0, \quad |\xi| < 1, \end{aligned} \quad (5.12)$$

$$\sum_{n=0}^N c_n \int_{-1}^1 P_n^{(\chi, \omega)}(\xi) w(\xi) d\xi = \frac{P}{\delta}, \quad (5.13)$$

where $A_1 = 2\mu_3/(\kappa + 1)$ and $A_2 = (\kappa + 1)/4\mu_1$, $U_n(\xi)$ are Chebyshev polynomials of the second kind, and the functions $H_n^{ij}(\xi)$, $i, j = 1, 2, 3$, are given by

$$H_n^{ij}(\xi) = c \int_{-1}^1 \tilde{k}_{ij}(\xi, \eta) \frac{T_n(\eta)}{\sqrt{1-\eta^2}} d\eta, \quad (i, j) = (1, 1), (1, 2), (2, 1), (2, 2), \quad (5.14)$$

$$H_n^{13}(\xi) = \delta \int_{-1}^1 [\tilde{g}_{11}(\xi, \eta) + \mu_f \tilde{g}_{12}(\xi, \eta)] P_n^{(\chi, \omega)}(\eta) w(\eta) d\eta, \quad (5.15)$$

$$H_n^{23}(\xi) = \delta \int_{-1}^1 [\tilde{g}_{21}(\xi, \eta) + \mu_f \tilde{g}_{22}(\xi, \eta)] P_n^{(\chi, \omega)}(\eta) w(\eta) d\eta, \quad (5.16)$$

$$H_n^{ij}(\xi) = c \int_{-1}^1 \tilde{g}_{ij}(\xi, \eta) \frac{T_n(\eta)}{\sqrt{1-\eta^2}} d\eta, \quad (i, j) = (3, 1), (3, 2), \quad (5.17)$$

$$H_n^{33}(\xi) = \delta \int_{-1}^1 [\tilde{k}_{31}(\xi, \eta) + \mu_f \tilde{k}_{32}(\xi, \eta)] P_n^{(\chi, \omega)}(\eta) w(\eta) d\eta, \quad (5.18)$$

in which it is noted that the logarithmic and signum functions involved in equation (5.14) can be treated by means of the following formulae (Gradshteyn & Ryzhik 1980):

$$\frac{1}{\pi} \int_{-1}^1 \frac{T_n(\eta)}{\sqrt{1-\eta^2}} \ln |\eta - \xi| d\eta = -\frac{1}{n} T_n(\xi), \quad n \geq 1, |\xi| < 1, \quad (5.19)$$

$$\int_{-1}^1 \frac{T_n(\eta)}{\sqrt{1-\eta^2}} \frac{|\eta - \xi|}{\eta - \xi} d\eta = \frac{2}{n} U_{n-1}(\xi) \sqrt{1-\xi^2}, \quad n \geq 1, |\xi| < 1. \quad (5.20)$$

In order to recast the functional equations (5.10)–(5.13) into solvable form, the orthogonal relations of $U_n(\xi)$ and $P_n^{(\chi, \omega)}(\xi)$ are utilized such that a system of linear algebraic equations is constructed for the unknown coefficients, a_n , b_n , $1 \leq n \leq N$ and c_n , $0 \leq n \leq (N + 1)$ as

$$\frac{\pi}{2} A_1 a_k + \sum_{n=1}^N Y_{kn}^{11} a_n + \sum_{n=1}^N Y_{kn}^{12} b_n + \sum_{n=0}^N Y_{kn}^{13} c_n = 0, \quad 1 \leq k \leq N, \quad (5.21)$$

$$\frac{\pi}{2} A_1 b_k + \sum_{n=1}^N Y_{kn}^{21} a_n + \sum_{n=1}^N Y_{kn}^{22} b_n + \sum_{n=0}^N Y_{kn}^{23} c_n = 0, \quad 1 \leq k \leq N, \quad (5.22)$$

$$-\frac{A_2}{2 \sin \pi \chi} \theta_k^{(-\chi, -\omega)} c_{k+1} + \sum_{n=1}^N Y_{kn}^{31} a_n + \sum_{n=1}^N Y_{kn}^{32} b_n + \sum_{n=0}^N Y_{kn}^{33} c_n = 0, \quad 0 \leq k \leq N, \quad (5.23)$$

$$c_0 = -\frac{P \sin \pi \chi}{\delta \pi}, \quad (5.24)$$

together with the definitions expressed as

$$Y_{kn}^{ij} = \int_{-1}^1 H_n^{ij}(\xi) U_{k-1}(\xi) \sqrt{1 - \xi^2} d\xi, \quad (i, j) = (1, 1), (1, 2), (1, 3), (2, 1), (2, 2), (2, 3), \quad (5.25)$$

$$Y_{kn}^{ij} = \int_{-1}^1 H_n^{ij}(\xi) P_k^{(-\chi, -\omega)}(\xi) (1 - \xi)^{-\chi} (1 + \xi)^{-\omega} d\xi, \quad (i, j) = (3, 1), (3, 2), (3, 3), \quad (5.26)$$

$$\theta_k^{(\chi, \omega)} = \begin{cases} \frac{\Gamma(k + \chi + 1)\Gamma(k + \omega + 1)}{2(k!)^2}, & k \geq 1, \\ \Gamma(\chi + 1)\Gamma(\omega + 1), & k = 0. \end{cases} \quad (5.27)$$

Once the coefficients, a_n , b_n and c_n , are evaluated from equations (5.21)–(5.24), the integral equations (4.7) and (4.8) can serve to provide the values of tractions, $\sigma_{3xx}(0, y)$ and $\sigma_{3xy}(0, y)$, ahead of the crack tips $|y| > c$. The singular terms of crack-tip tractions, in conjunction with equations (5.3), (5.5) and (5.6), are then obtained as

$$\begin{Bmatrix} \sigma_{3xx}(0, \xi) \\ \sigma_{3xy}(0, \xi) \end{Bmatrix} = -\frac{2\mu_3}{1 + \kappa} \sum_{n=1}^N \begin{Bmatrix} a_n \\ b_n \end{Bmatrix} \frac{[\xi - \text{sgn}(\xi)\sqrt{\xi^2 - 1}]^n}{\text{sgn}(\xi)\sqrt{\xi^2 - 1}} + O(1), \quad |\xi| > 1, \quad (5.28)$$

where $O(\cdot)$ denotes the non-singular terms involving the bounded kernels and the contact pressure distribution beneath the flat punch can be determined in a straightforward manner as

$$\begin{aligned} \sigma_{1xx}(0, y) = -\phi_3(y) = -2\sigma_0 \left(\frac{\delta + e - y}{\delta} \right)^{\chi} \left(\frac{\delta - e + y}{\delta} \right)^{\omega} \\ \times \sum_{n=0}^{N+1} c_n^* P_n^{(\chi, \omega)} \left(\frac{y - e}{\delta} \right), \quad |y - e| < \delta, \end{aligned} \quad (5.29)$$

in which $\sigma_0 = p/2\delta$ is the average contact pressure and $c_n^* = \delta c_n/P$.

Moreover, the expression for the in-plane stress component, $\sigma_{1yy}(0, y)$, acting on the coating surface is obtainable from the constitutive equations (2.4)–(2.6) and equation (4.4) such that

$$\begin{aligned} \sigma_{1yy}(0, y) = -\phi_3(y) + \frac{2\mu_f}{\pi} \int_{e-\delta}^{e+\delta} \frac{\phi_3(r)}{r - y} dr \\ + \frac{8\mu_1}{1 + \kappa} \int_{e-\delta}^{e+\delta} [k_{41}(y, r) + \mu_f k_{42}(y, r)] \phi_3(r) dr \\ + \frac{8\mu_1}{1 + \kappa} \int_{-c}^c \sum_{j=1}^2 g_{4j}(y, r) \phi_j(r) dr, \quad |y| < \infty, \end{aligned} \quad (5.30)$$

where $k_{4j}(y, r)$ and $g_{4j}(y, r)$, $j = 1, 2$, are the kernels which are also bounded as

$$k_{41}(y, r) = \frac{1}{\pi} \int_0^\infty [sN_{21}(s) - N_2^\infty] \cos s(r - y) ds, \quad (5.31)$$

$$k_{42}(y, r) = -\frac{1}{\pi} \int_0^\infty [sN_{22}(s) - N_1^\infty] \sin s(r - y) ds, \quad (5.32)$$

$$g_{41}(y, r) = -\frac{1}{\pi} \int_0^\infty P_{21}(s) \sin s(r - y) ds, \quad (5.33)$$

$$g_{42}(y, r) = -\frac{1}{\pi} \int_0^\infty P_{22}(s) \cos s(r - y) ds, \quad (5.34)$$

and in particular, in the normalized interval of $r = e + \delta\eta$ and $y = e + \delta\xi$, the second term on the right-hand side in equation (5.30) can be evaluated via the formula given by (Erdogan 1978)

$$L_n(\xi) = \int_{-1}^{+1} \frac{w(\eta)P_n^{(\chi, \omega)}(\eta)}{\eta - \xi} d\eta, \quad |\xi| < \infty, \quad (5.35)$$

along with the following recurrence relation:

$$L_{n+1}(\xi) = \frac{1}{P_n^{(\chi, \omega)}(\xi)} \left[P_{n+1}^{(\chi, \omega)}(\xi)L_n(\xi) + \frac{2n+1}{n+1}\theta_n^{(\chi, \omega)} \right], \quad n \geq 0, \quad (5.36)$$

$$L_0(\xi) = \frac{\pi}{\sin \pi \chi} \begin{cases} (\xi - 1)^\chi (\xi + 1)^\omega, & |\xi| > 1, \\ (1 - \xi)^\chi (1 + \xi)^\omega \cos \pi \chi, & |\xi| < 1. \end{cases} \quad (5.37)$$

From the structure of the crack-tip singular tractions in equation (5.28), as the physical quantities of primary interest in fracture analysis, the mixed-mode stress intensity factors are defined and evaluated in terms of the solution to the integral equations such that

$$\begin{Bmatrix} K_I(-c) \\ K_{II}(-c) \end{Bmatrix} \equiv \lim_{y \rightarrow -c^-} \sqrt{2(-y - c)} \begin{Bmatrix} \sigma_{3xx}(0, y) \\ \sigma_{3xy}(0, y) \end{Bmatrix} = \frac{2\mu_3\sqrt{c}}{\kappa + 1} \sum_{n=1}^N (-1)^n \begin{Bmatrix} a_n \\ b_n \end{Bmatrix}, \quad (5.38)$$

$$\begin{Bmatrix} K_I(+c) \\ K_{II}(+c) \end{Bmatrix} \equiv \lim_{y \rightarrow +c^+} \sqrt{2(y - c)} \begin{Bmatrix} \sigma_{3xx}(0, y) \\ \sigma_{3xy}(0, y) \end{Bmatrix} = -\frac{2\mu_3\sqrt{c}}{\kappa + 1} \sum_{n=1}^N \begin{Bmatrix} a_n \\ b_n \end{Bmatrix}, \quad (5.39)$$

where K_I and K_{II} are modes I and II stress intensity factors, respectively. Furthermore, in order to give a quantitative measure of the severity of the contact pressure singularities at the edges of the flat punch, similar to the concept used for characterizing the local crack-tip response, the punch-edge stress intensity factors are defined and evaluated as

$$K_T = \lim_{y \rightarrow e - \delta} \phi_3(y)(\delta - e + y)^{-\omega} = K_{0T} \sum_{n=0}^{N+1} c_n^* P_n^{(\chi, \omega)}(-1), \quad (5.40)$$

$$K_L = \lim_{y \rightarrow e + \delta} \phi_3(y)(\delta + e - y)^{-\chi} = K_{0L} \sum_{n=0}^{N+1} c_n^* P_n^{(\chi, \omega)}(+1), \quad (5.41)$$

in which $K_{0T} = \sigma_0(2\delta)^{-\omega}$ and $K_{0L} = \sigma_0(2\delta)^{-\chi}$ are the normalizing factors, and the suffix T refers to the trailing edge of the punch ($y = e - \delta$) and the suffix L is for the leading edge of the punch ($y = e + \delta$).

It should now be pointed out that, as will be illustrated in the next section, under the compressive contact stress field imposed by the sliding punch, the values of mode I stress intensity factors are obtained to be negative with the implication of the crack closure and the ensuing possibility of crack-face contact and friction, thereby invalidating the traction-free conditions in equation (2.11). In the present study, however, the contact and friction between the closed crack faces are not taken into account.

6. Results and discussion

Numerical results are generated to investigate the interactions between the contact stress field and the crack-tip behaviour for various combinations of material, geometric and loading parameters of the coated system (see figures 2–6, and figures 7–13 in the electronic supplementary material). The state of plane strain is assumed with a constant Poisson's ratio $\nu = 0.3$. The integrals in equations (5.14)–(5.18), (5.25) and (5.26) are evaluated based on the Gauss–Chebyshev or Gauss–Jacobi quadrature rules, whereas the improper integrals in equations (4.10)–(4.21) and (5.31)–(5.34) are evaluated employing the Gauss–Legendre quadrature rule (Davis & Rabinowitz 1984), with 26-term expansions of the Chebyshev and Jacobi polynomials in equations (5.5)–(5.7). The resulting values of mixed-mode stress intensity factors are normalized by $K_0 = \sigma_0 c^{1/2}$. It should be noted that, for verification and validation purposes, some of the results due to Guler & Erdogan (2004) and Choi & Paulino (2008) for the contact of graded coatings can be reproduced when c/δ approaches zero or e/c is sufficiently large, as a limiting case of the present coupled formulation and numerical implementation. Likewise, by letting δ/c be very small and e/c be also sufficiently large, and applying the uniform crack-face tractions in equation (2.11), the near-tip solutions corresponding to the pressurized interface crack can be generated which coincide with those available in the literature (Erdogan 1998).

The effect of the presence of an interface crack on the contact stress field is first examined. To this end, the crack length relative to the punch width, c/δ , is taken to be a variable and the other parameters are set as $\mu_f = 0.5$, $h_1/h = h_2/h = 0.5$ and $\delta/h = 0.5$, with the punch being located at $e/c = 0$. Figures 2 and 3 illustrate the distributions of normalized contact stress $\sigma_{1xx}(0, y)/\sigma_0$ and in-plane surface stress $\sigma_{1yy}(0, y)/\sigma_0$ for $\mu_1/\mu_3 = 5.0$ and $\mu_1/\mu_3 = 0.2$, respectively. In this case, the powers of stress singularity at the leading ($y = e + \delta$) and the trailing ($y = e - \delta$) edges of the flat punch as determined from equation (5.8) are $\chi = -0.4548$ and $\omega = -0.5452$, respectively, resulting in the greater stress concentrations around the trailing edge of the punch. When the interfacial cracking is extended by increasing c/δ , it can be observed in figures 2*a* and 3*a* that there are also greater stress concentrations around both ends of the punch. The distributions of the in-plane stress component in figures 2*b* and 3*b*, which are discontinuous and unbounded at both edges of the punch, exhibit tensile responses just behind the trailing edge ($y < -\delta$) that may trigger the initiation and growth of surface cracking in load transfer components through the sliding contact

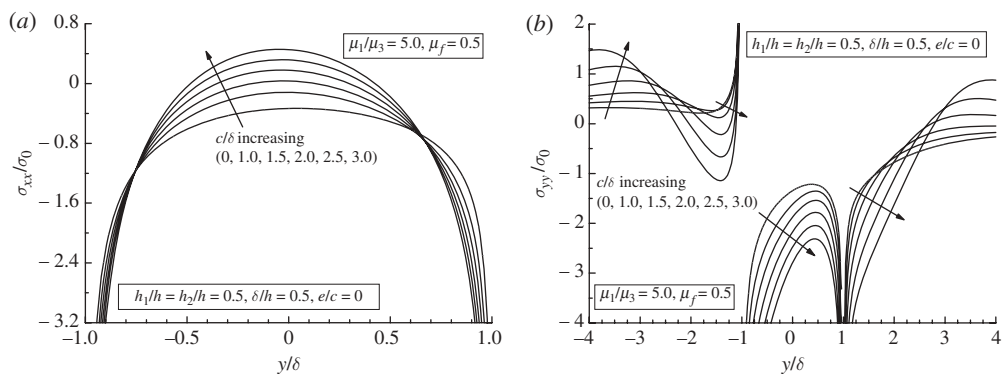


Figure 2. Effect of crack length c/δ on the distributions of (a) contact stress $\sigma_{1xx}(0, y)/\sigma_0$ and (b) in-plane surface stress $\sigma_{1yy}(0, y)/\sigma_0$ for shear modulus ratio $\mu_1/\mu_3 = 5.0$ ($\mu_f = 0.5$, $h_1/h = h_2/h = 0.5$, $\delta/h = 0.5$, $e/c = 0.0$, $\sigma_0 = P/2\delta$).

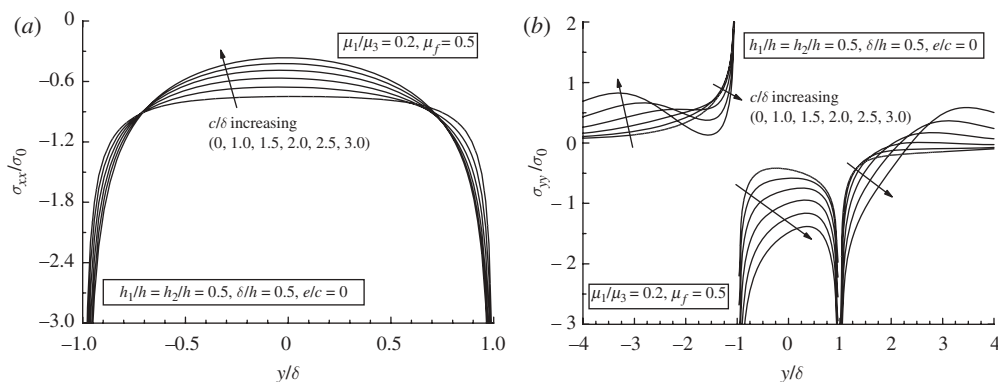


Figure 3. Effect of crack length c/δ on the distributions of (a) contact stress $\sigma_{1xx}(0, y)/\sigma_0$ and (b) in-plane surface stress $\sigma_{1yy}(0, y)/\sigma_0$ for shear modulus ratio $\mu_1/\mu_3 = 0.2$ ($\mu_f = 0.5$, $h_1/h = h_2/h = 0.5$, $\delta/h = 0.5$, $e/c = 0.0$, $\sigma_0 = P/2\delta$).

(Suresh 2001). In the remaining region of the coating surface, it is predicted that the in-plane surface stress is in general rendered greater as the relative crack size c/δ increases.

Of particular interest is that when the coating is stiffer, as $\mu_1/\mu_3 = 5.0$, and the crack length is greater than the punch width as, $c/\delta > 1.5$, in figure 2a, the contact stress is redistributed from that of $c/\delta = 0$ in such a noteworthy manner that it becomes tensile around the middle of the contact region, not fulfilling the complete contact condition between the flat punch and the coating surface in equation (2.12), but indicating the formation of local separation. With reference to the above stress response, it is appropriate to recall that Shield & Boggy (1989) examined the problem of a frictionless, flat punch contacting a layered half-plane and predicted the tensile contact stress and thus separation in some portion of the contact region, especially for the case of a stiffer layer bonded to a much softer half-plane. The local bending of the stiff surface layer was considered to

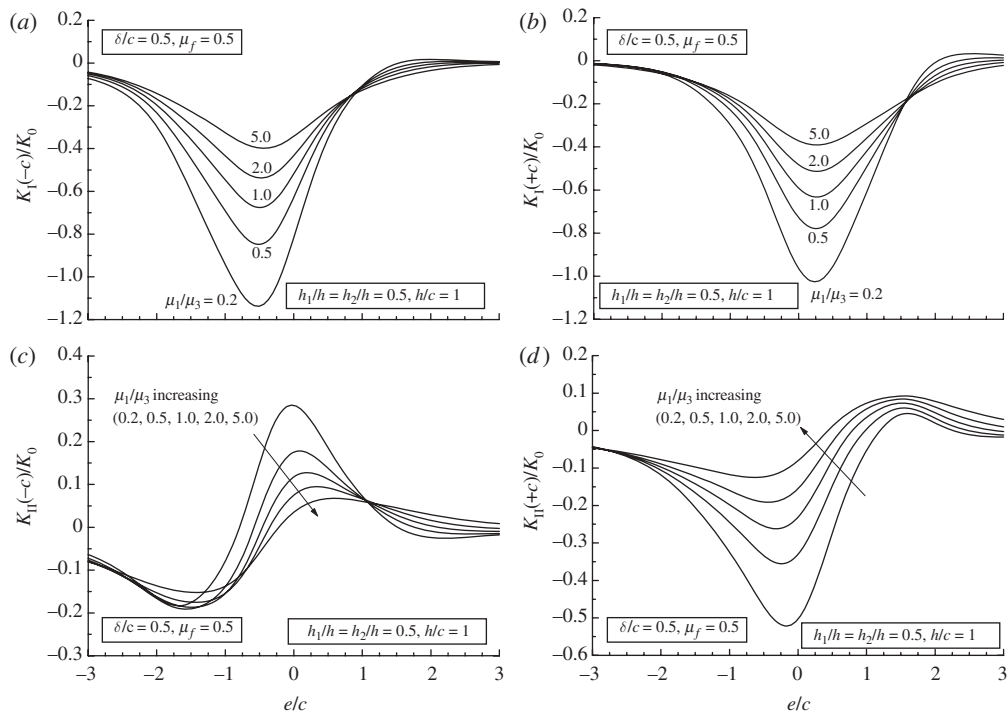


Figure 4. Variations of crack-tip stress intensity factors (a) $K_I(-c)/K_0$, (b) $K_I(+c)/K_0$, (c) $K_{II}(-c)/K_0$, and (d) $K_{II}(+c)/K_0$ versus punch location e/c for different values of shear modulus ratio μ_1/μ_3 ($\delta/c = 0.5$, $\mu_f = 0.5$, $h_1/h = h_2/h = 0.5$, $h/c = 1.0$, $K_0 = \sigma_0 c^{1/2}$, $\sigma_0 = P/2\delta$).

be largely responsible for the separation within the contact region. In the current coupled crack/contact problem, the presence of a relatively large interface crack is understood to play the additive role of enhancing such local bending behaviour of the stiff coating underneath the flat punch, together with the influence of the crack-induced compliance change in the coated system.

In the sequel, figure 4*a–d* compares the crack-tip behaviour for different values of shear modulus ratio μ_1/μ_3 , with the other parameters being fixed as $\delta/c = 0.5$, $\mu_f = 0.5$, $h_1/h = h_2/h = 0.5$ and $h/c = 1.0$, by plotting the variations of corresponding mixed-mode stress intensity factors K_I and K_{II} as a function of punch location e/c . A general observation made from these figures is that, for the given value of μ_1/μ_3 , the peak stress intensity factors are attained when the punch is acting around the crack centre and that the increases in the shear modulus ratio μ_1/μ_3 result in lowering the absolute values of stress intensity factors, especially when the punch is passing over the crack. Such a reduction is mainly due to the suppressed elastic deformation around the crack tips with the increased coating rigidity, accompanied by a lower likelihood of debonding.

It should be mentioned that, in figure 4*a,b*, the overall values of K_I during the passage of the punch are, as expected, found to be negative, implying closed crack faces under the compressive stress field and thus crack growth possibly in shear mode. If the interdigitated or interlocked profile across the actual

unextended crack faces were to take effect, however, in conjunction with the frictional resistance between them, such compressive stresses would hinder the mode II deformation around the crack tips, tending to prevent the crack growth in shear mode. The trajectory of the crack growth would then be affected by the values of K_{II} in such a way that the positive K_{II} may deflect or kink the crack in the clockwise direction, while the negative ones may cause the crack to also grow out of its plane in the counterclockwise direction, but depending on the relative magnitude of fracture toughness of the adjacent constituents. Otherwise, the crack may tend to grow along the line of the interface when the bonding lacks the necessary strength. For instance, when $\mu_1/\mu_3 = 0.2$, figure 4*c,d* depicts that the major values of K_{II} history experienced at each of the crack tips within the given range of e/c are different in their signs, with a consequence of probable crack growth in different directions leading to the crack branching toward the surface of the coated system. It should be noted that the negative mode I stress intensification becomes positive at both the crack tips when the coating layer is much less stiff than the substrate, as $\mu_1/\mu_3 = 0.2$, and the punch is acting to the far right of the crack, as $e/c = 2.0$.

As mentioned above, the negative values of K_I in figure 4*a,b* and in the other figures that follow are indicative of the crack closure under the interacting sliding contact-induced stress field, together with the existence of unknown contact and frictional stresses between the crack faces. If the crack-face contact and friction were taken into account, the incumbent problem would become highly nonlinear and more complicated. In consideration of the processing-induced internal stress gradients, however, that may be residing inside the coated medium (Kesler *et al.* 1997) and within the context of linear elasticity, the effect of any pre-existing residual stresses can be superimposed on the present solutions. The negative values of K_I in this study can then be applicable when the superposition with uncoupled solutions due to the large enough residual and/or other external tensile stresses gives rise to the positive resultant K_I and thus keeps the crack open at any load.

To be addressed subsequently is the assessment of criticality resulting from the singular nature of the contact pressure distributions around a flat punch in terms of the punch-edge stress intensity factors, K_T and K_L , as evaluated from equations (5.40) and (5.41) and plotted in figure 5*a,b*. The singular stresses at the punch edges therein are predicted to be intensified as the shear modulus ratio μ_1/μ_3 becomes greater, as opposed to those at the crack tips. In addition, the values of such punch-edge stress intensity factors at the trailing edge arrive at the peaks when the punch is acting on the location of the left-hand half of the crack, while those at the leading edge attain their peaks when the punch is acting on the right-hand half of the crack. In comparison, the severity of singular stresses in the close vicinity of punch edges is seen to be slightly greater at the leading edge than at the trailing edge, which is also in contrast to the case in which there is no crack (Choi & Paulino 2008).

The variations in crack-tip stress intensity factors K_I and K_{II} with distance e/c behind the punch centreline are shown in figure 6*a–d* for different interlayer thicknesses h_2/h and shear modulus ratios μ_1/μ_3 . The other geometric parameters are specified as $h/c = 1.0$, $\delta/c = 0.5$, with the friction coefficient being $\mu_f = 0.5$. It is then observed that, for the stiff coating with $\mu_1/\mu_3 = 5.0$, the increase in the thickness of the graded interlayer has a tendency to augment the stress intensity

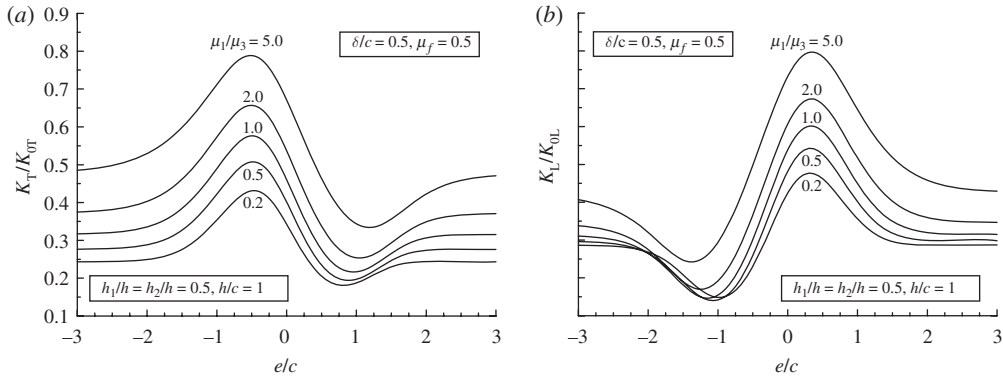


Figure 5. Variations of punch-edge stress intensity factors (a) K_T/K_{0T} and (b) K_L/K_{0L} versus punch location e/c for different values of shear modulus ratio μ_1/μ_3 ($\delta/c = 0.5$, $\mu_f = 0.5$, $h_1/h = h_2/h = 0.5$, $h/c = 1.0$, $K_{0T} = \sigma_0(2\delta)^{-\omega}$, $K_{0L} = \sigma_0(2\delta)^{-\lambda}$, $\sigma_0 = P/2\delta$).

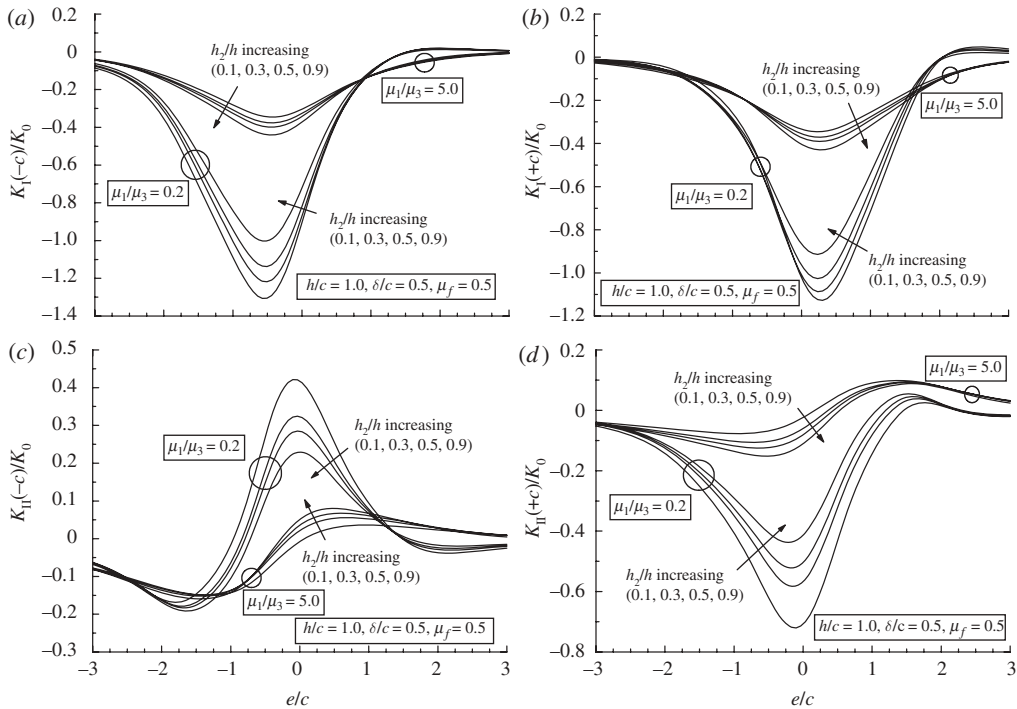


Figure 6. Variations of crack-tip stress intensity factors (a) $K_{I(-c)}/K_0$, (b) $K_{I(+c)}/K_0$, (c) $K_{II(-c)}/K_0$, and (d) $K_{II(+c)}/K_0$ versus punch location e/c for different values of interlayer thickness h_2/h and shear modulus ratio μ_1/μ_3 ($h/c = 1.0$, $\delta/c = 0.5$, $\mu_f = 0.5$, $K_0 = \sigma_0 c^{1/2}$, $\sigma_0 = P/2\delta$).

factors, while the reverse effect of the interlayer prevails for the compliant coating with $\mu_1/\mu_3 = 0.2$. Such a trend with h_2/h indicates that the thinner graded interlayer for the stiff coating, to some extent, would be more effective in shielding the tip behaviour of the interface crack, and, for the compliant coating, the thinner

interlayer would have the adverse influence of intensifying the crack-tip severity under the interacting contact stress field. The results also predict that, when the punch is located to the right of the crack and $\mu_1/\mu_3 = 0.2$, the closed crack faces may open, although the effect of h_2/h on this crack opening is not significant. In addition, figure 7*a,b* in the electronic supplementary material plots the variations of punch-edge stress intensity factors, K_T and K_L . It is then demonstrated that, for the stiff coating, the state of punch-edge stresses becomes more severe with the increasing interlayer thickness h_2/h , whereas the state of such stresses is relaxed with h_2/h for the compliant coating.

The effect of the homogeneous coating thickness, h_1/c , on the crack-tip is examined in figure 8*a–d* in the electronic supplementary material for $\mu_1/\mu_3 = 5.0$, $\mu_f = 0.5$, $h_2/c = 0.5$ and $\delta/c = 0.5$. A notable feature is that, for the thinner coating that may correspond to a relatively long and shallow crack, due to the enlarged interactions with the contact stress field, the values of both K_I and K_{II} are of greater magnitude. Figure 8*c,d* in the electronic supplementary material also delineates that, when the coating is as thin as $h_1/c = 0.2$ and the punch is approaching the crack from the left-hand side, the values of K_{II} are going through the negative peaks, accelerating the crack growth in shear mode. It should be pointed out that the effect of increasing h_1/c is quite compatible with that of increasing the coating stiffness, as was illustrated in figure 4*a–d*. Moreover, the results in figure 9*a,b* in the electronic supplementary material show that the punch-edge stress intensifications, K_T and K_L , are markedly amplified when the punch passes over the crack and the coating thickness is less than the crack length, mainly caused by the greater interactions with the crack-tip stress field.

Figure 10*a–d* in the electronic supplementary material further demonstrates how the punch width, δ/c , affects the tip behaviour of the interface crack, where the results are for $\mu_1/\mu_3 = 5.0$, $\mu_f = 0.5$, $h_1/h = h_2/h = 0.5$ and $h/c = 1.0$. In this case, the magnitudes of K_I and K_{II} are, as expected, undergoing substantial increases for the greater punch width. Likewise, the state of punch-edge singular stresses in terms of K_T and K_L is shown to be intensified for the greater punch width, as can be observed in figure 11*a,b* in the electronic supplementary material. It should be pointed out that the overall effect of increasing the punch width is quite similar to that of decreasing the coating thickness.

With the friction coefficient μ_f being chosen to vary in the range of 0–0.9, figure 12*a–d* in the electronic supplementary material illustrates the variations of crack-tip stress intensity factors versus punch locations e/c , along with $\mu_1/\mu_3 = 5.0$, $\delta/c = 0.5$, $h_1/h = h_2/h = 0.5$ and $h/c = 1.0$. In figure 12*a,b* in the electronic supplementary material, the closed crack faces at all punch locations are also revealed for the given values of the friction coefficient. As the sliding contact between the punch and the coating surface becomes more frictional, it is further observed that the values of both K_I and K_{II} are rendered greater when the punch is approaching the crack, but reduced when the punch is sliding away from the crack, such that the effect of the friction is to increase the closure of the crack faces for $e/c < 0$ and to decrease the closure for $e/c > 0$. In figure 13*a,b* in the electronic supplementary material, however, during the more frictional passage of the punch, the values of punch-edge stress intensity factors at the trailing edge K_T become greater as the punch approaches and leaves the crack tips, whereas those at the leading edge K_L yield the reverse trend.

7. Closure

The problem of a coupled crack/contact mechanics has been investigated for a coating/substrate system with functionally graded properties, in the context of linear plane elasticity. The graded material was modelled as a non-homogeneous interlayer in the coated system that was loaded by a frictional sliding flat punch and the crack was assumed to exist along the interface between the interlayer and the substrate. With the derivation of a set of three simultaneous Cauchy-type singular integral equations for the coupled mixed boundary value problem, the strong interactions between the contact stress field and the crack-tip behaviour were addressed by evaluating the crack-tip and punch-edge stress intensity factors as well as the contact stress distributions for various combinations of material, geometric and loading parameters of the coated medium. It is worth noting that the analysis of the coupled fracture and contact problem considered herein could become more intricate by a crack closure with unknown contact and frictional stresses between the crack faces, under the influence of a sliding contact-induced stress field that is predominantly compressive. The crack-face contact and friction may be dealt with by using a Coulomb friction model, which assumes an instantaneous dependence between normal and shear stresses. Nonetheless, incorporation of such complicating factors that require further elaboration was not simulated in the present work, in the sense that the crack closure is what may occur in reality under the compressive stress field and the corresponding negative values of mode I stress intensification could still be useful, provided superposition with those arising from large enough residual and/or remote tensile loading keeps the crack open at any punch locations.

References

- Bahar, L. Y. 1972 Transfer matrix approach to layered system. *ASCE J. Eng. Mech.* **98**, 1159–1172.
- Bower, A. F. & Fleck, N. A. 1994 Brittle fracture under a sliding line contact. *J. Mech. Phys. Solids* **42**, 1375–1396. (doi:10.1016/0022-5096(94)90002-7)
- Bryant, M. D., Miller, G. R. & Keer, L. M. 1984 Line contact between a rigid indenter and a damaged elastic body. *Quart. J. Mech. Appl. Math.* **37**, 467–478. (doi:10.1093/qjmam/37.3.467)
- Chan, Y.-S., Paulino, G. H. & Fannjiang, A. C. 2008 Gradient elasticity theory for mode III fracture in functionally graded materials—part II: crack parallel to the material gradation. *ASME J. Appl. Mech.* **75**, 061015-1–061015-11.
- Choi, H. J. 2001a The problem for bonded half-planes containing a crack at an arbitrary angle to the graded interfacial zone. *Int. J. Solids Struct.* **38**, 6559–6588. (doi:10.1016/S0020-7683(01)00090-7)
- Choi, H. J. 2001b Effects of graded layering on the tip behavior of a vertical crack in a substrate under frictional Hertzian contact. *Eng. Fract. Mech.* **68**, 1033–1059. (doi:10.1016/S0013-7944(01)00003-0)
- Choi, H. J. 2003 Thermoelastic problem of steady-state heat flow disturbed by a crack perpendicular to the graded interfacial zone in bonded materials. *J. Therm. Stresses* **26**, 997–1030. (doi:10.1080/01495730306341)
- Choi, H. J. 2004 Impact response of a surface crack in a coating/substrate system with a functionally graded interlayer: antiplane deformation. *Int. J. Solids Struct.* **41**, 5631–5645. (doi:10.1016/j.ijsolstr.2004.04.020)
- Choi, H. J. 2006 Elastodynamic analysis of a crack at an arbitrary angle to the graded interfacial zone in bonded half-planes under antiplane shear impact. *Mech. Res. Commun.* **33**, 636–650. (doi:10.1016/j.mechrescom.2005.05.009)

- Choi, H. J. 2007a Stress intensity factors for an oblique edge crack in a coating/substrate system with a graded interfacial zone under antiplane shear. *Eur. J. Mech. A: Solids* **26**, 337–347. (doi:10.1016/j.euromechsol.2006.06.004)
- Choi, H. J. 2007b Impact behavior of an inclined edge crack in a layered medium with a graded nonhomogeneous interfacial zone: antiplane deformation. *Acta Mech.* **193**, 67–84. (doi:10.1007/s00707-007-0475-3)
- Choi, H. J. & Paulino, G. H. 2008 Thermoelastic contact mechanics for a flat punch sliding over a graded coating/substrate system with frictional heat generation. *J. Mech. Phys. Solids* **56**, 1673–1692. (doi:10.1016/j.jmps.2007.07.011)
- Dag, S. 2006 Thermal fracture analysis of orthotropic functionally graded materials using an equivalent domain integral approach. *Eng. Fract. Mech.* **73**, 2802–2828. (doi:10.1016/j.engfracmech.2006.04.015)
- Dag, S. & Erdogan, F. 2002 A surface crack in a graded medium loaded by a sliding rigid stamp. *Eng. Fract. Mech.* **69**, 1729–1751. (doi:10.1016/S0013-7944(02)00053-X)
- Davis, P. J. & Rabinowitz, P. 1984 *Methods of numerical integration*, 2nd edn. New York: Academic Press.
- Eischen, J. W. 1987 Fracture of nonhomogeneous materials. *Int. J. Fract.* **34**, 3–22.
- El-Borgi, S., Keer, L. M. & Said, W. B. 2004 An embedded crack in a functionally graded coating bonded to a homogeneous substrate under frictional Hertzian contact. *Wear* **257**, 760–776. (doi:10.1016/j.wear.2004.03.016)
- Erdogan, F. 1978 Mixed boundary value problems in mechanics. In *Mechanics today*, vol. 4 (ed. S. Nemat-Nasser), pp. 1–86. New York, NY: Pergamon Press.
- Erdogan, F. 1998 Crack problems in nonhomogeneous materials. In *Fracture, a topical encyclopedia of current knowledge* (ed. G. P. Cherepanov), pp. 72–98. Malabar, FL: Krieger.
- Erdogan, F. & Ozturk, M. 2008 On the singularities in fracture and contact mechanics. *ASME J. Appl. Mech.* **75**, 051111-1–051111-12.
- Friedman, B. 1991 *Lectures on application-oriented mathematics*. New York, NY: John Wiley & Sons.
- Gradshteyn, I. S. & Ryzhik, I. M. 1980 *Table of integrals, series, and products*. New York, NY: Academic Press.
- Guler, M. A. & Erdogan, F. 2004 Contact mechanics of graded coatings. *Int. J. Solids Struct.* **41**, 3865–3889. (doi:10.1016/j.ijsolstr.2004.02.025)
- Hasebe, N., Okumura, M. & Nakamura, T. 1989 Frictional punch and crack in plane elasticity. *ASCE J. Eng. Mech.* **115**, 1137–1149. (doi:10.1061/(ASCE)0733-9399(1989)115:6(1137))
- Hills, D. A., Nowell, D. & Sackfield, A. 1993 *Mechanics of elastic contacts*. Oxford, UK: Butterworth-Heinemann.
- Jin, Z.-H. & Noda, N. 1994 Crack-tip singular fields in nonhomogeneous materials. *ASME J. Appl. Mech.* **61**, 738–740.
- Jitcharoen, J., Pature, N., Giannakopoulos, A. E. & Suresh, S. 1998 Hertzian-crack suppression in ceramics with elastic-modulus-graded surface. *J. Am. Ceram. Soc.* **81**, 2301–2308.
- Ke, L.-L. & Wang, Y.-S. 2007 Two-dimensional sliding frictional contact of functionally graded materials. *Eur. J. Mech. A: Solids* **26**, 171–188. (doi:10.1016/j.euromechsol.2006.05.007)
- Keer, L. M., Bryant, M. D. & Haritos, G. K. 1982 Subsurface and surface cracking due to Hertzian contact. *ASME J. Lubr. Tech.* **104**, 347–351.
- Kesler, O., Finot, M., Suresh, S. & Sampath, S. 1997 Determination of processing-induced stresses and properties of layered and graded coatings: experimental method and results for plasma-sprayed Ni-Al₂O₃. *Acta Mater.* **45**, 3123–3134. (doi:10.1016/S1359-6454(97)00015-3)
- Lee, H.-J. & Choi, H. J. 2006 Effects of graded properties on the impact response of an interface crack in a coating/substrate system subjected to antiplane deformation. *Z. Angew. Math. Mech.* **86**, 110–119. (doi:10.1002/zamm.200410221)
- Lee, Y.-D. & Erdogan, F. 1998 Interface cracking of FGM coatings under steady-state heat flow. *Eng. Fract. Mech.* **59**, 361–380. (doi:10.1016/S0013-7944(97)00137-9)
- Munisamy, R. L., Hills, D. A. & Nowell, D. 1995 An analysis of coupling between plane cracks and contacts. *Eur. J. Mech. A: Solids* **14**, 55–71.

- Muskhelishvili, N. I. 1953 *Singular integral equations*. Groningen, The Netherlands: Noordhoff.
- Oliveira, S. A. G. & Bower, A. F. 1996 An analysis of fracture and delamination in thin coatings subjected to contact loading. *Wear* **198**, 15–32. (doi:10.1016/0043-1648(95)06885-6)
- Paulino, G. H., Chan, Y.-S. & Fannjiang, A. C. 2003 Gradient elasticity theory for mode III fracture in functionally graded materials—part I: crack perpendicular to the material gradation. *ASME J. Appl. Mech.* **70**, 531–542.
- Rice, J. R. 1988 Elastic fracture mechanics concepts for interfacial cracks. *ASME J. Appl. Mech.* **55**, 98–103.
- Schulz, U., Peters, M., Bach, F.-W. & Tegereder, G. 2003 Graded coatings for thermal, wear and corrosion barriers. *Mater. Sci. Eng.* **A362**, 61–80. (doi:10.1016/S0921-5093(03)00579-3)
- Shield, T. W. & Bogy, D. B. 1989 Multiple region contact solutions for a flat indenter on a layered elastic half space: plane-strain case. *ASME J. Appl. Mech.* **56**, 251–262.
- Song, S. H. & Paulino, G. H. 2006 Dynamic stress intensity factors for homogeneous and smoothly heterogeneous materials using the interaction integral method. *Int. J. Solids Struct.* **43**, 4830–4866. (doi:10.1016/j.ijsolstr.2005.06.102)
- Suresh, S. 2001 Graded materials for resistance to contact deformation and damage. *Science* **292**, 2447–2451. (doi:10.1126/science.1059716)
- Suresh, S., Giannakopoulos, A. E. & Alcala, J. 1997 Spherical indentation of compositionally graded materials: theory and experiments. *Acta Mater.* **45**, 1307–1321. (doi:10.1016/S1359-6454(96)00291-1)
- Walters, M. C., Paulino, G. H. & Dodds Jr, R. H. 2004 Stress-intensity factors for surface cracks in functionally graded materials under mode-I thermomechanical loading. *Int. J. Solids Struct.* **41**, 1081–1118. (doi:10.1016/j.ijsolstr.2003.09.050)
- Zalounina, A. A. & Andreasen, J. H. 2004 A cracked coated solid subjected to contact loading. *Wear* **257**, 671–686. (doi:10.1016/j.wear.2004.02.008)